Cell Stem Cell, Volume *25*

Supplemental Information

Cardiac Reprogramming Factors Synergistically Activate Genome-wide Cardiogenic Stage-Specific Enhancers

Hisayuki Hashimoto, Zhaoning Wang, Glynnis A. Garry, Venkat S. Malladi, Giovanni A. Botten, Wenduo Ye, Huanyu Zhou, Marco Osterwalder, Diane E. Dickel, Axel Visel, Ning Liu, Rhonda Bassel-Duby, and Eric N. Olson

Supplemental Information

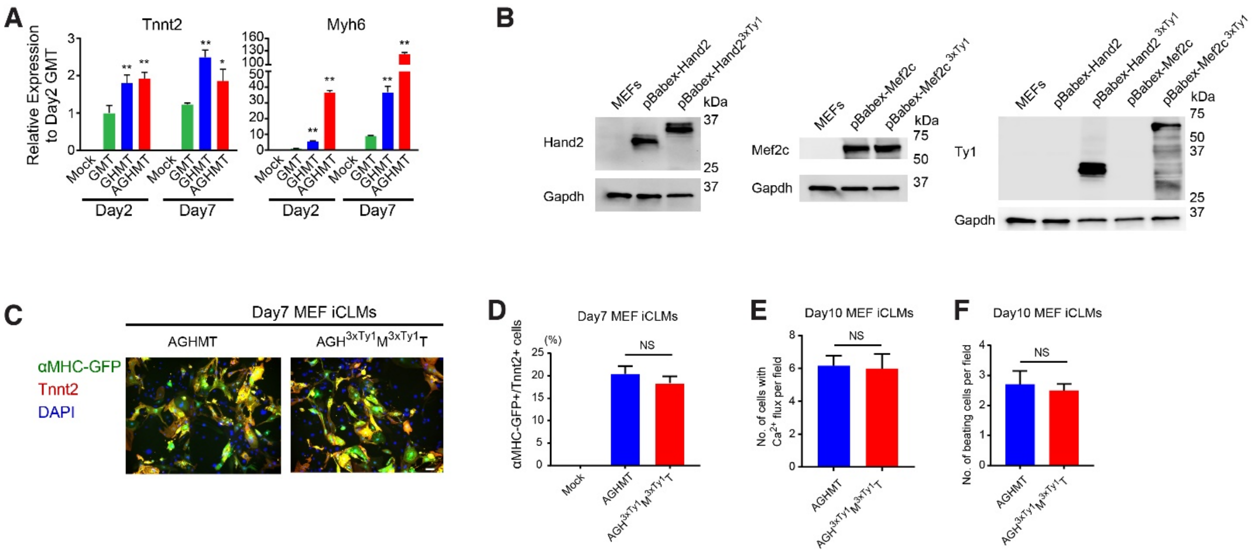

Figure S1, related to Figure 1. Cardiac Reprogramming by Tagged Reprogramming Factors.

(A) Transcript levels of Tnnt2 and Myh6 were increased 2 days after induction by adding Hand2 and Akt1 to GMT in MEFs. Transcript levels are normalized to Gapdh (n = 3, independent experiments). (* $P< 0.05$ vs. GMT, ** $P< 0.01$ vs. GMT). Data represented as mean ± SD.

(B) Western blot of 3xTy1 tagged Hand2 and Mef2c expressed in HEK293 cells.

(C) Representative immunocytochemistry images of day 7 αMHC-GFP transgenic MEFs treated with AGHMT or AGH^{3xTy1}M^{3xTy1}T. Cells were fixed and stained for αMHC-GFP (green), Tnnt2 (red), and DAPI (blue) 7 days after infection. Bars, 100 um.

(D) Quantification by flow cytometry of αMHC-GFP+ and Tnnt2+ iCLMs 7 days after infection with AGHMT or AGH^{3xTy1}M^{3xTy1}T (n = 3, independent experiments). Data represented as mean ± SD.

(E) Quantification of Ca^{2+} flux-positive MEFs after 10 days of reprogramming using Fluo-4 NW dye (n = 3, independent experiments). Data represented as mean ± SD.

(F) Quantification of spontaneous beating iCLMs 10 days after reprogramming (n = 3, independent experiments). Data represented as mean ± SD.

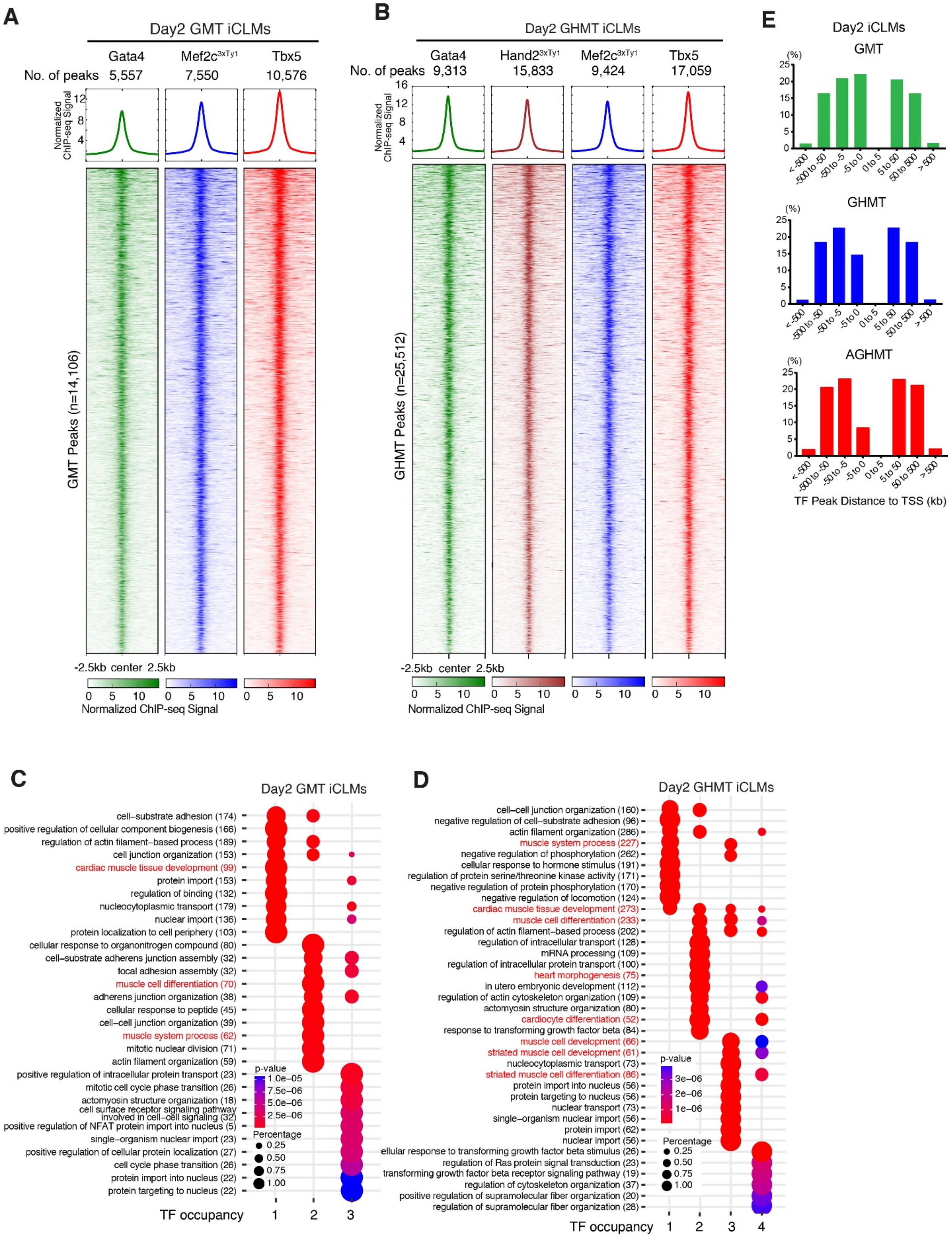
A
Day2 GMT iCLMs
Gata4
Mef2c^{3xTy1}
Tbx5
No. of peaks
5,557
7,550
10,576
Normalized ChIP-seq Signal
12
8
4
GMT Peaks (n=14,106)
-2.5kb center 2.5kb
0 5 10
0 5 10
0 5 10
Normalized ChIP-seq Signal
B
Day2 GHMT iCLMs
Gata4
Hand2^{3xTy1}
Mef2c^{3xTy1}
Tbx5
No. of peaks
9,313
15,833
9,424
17,059
Normalized ChIP-seq Signal
16
12
8
4
GHMT Peaks (n=25,512)
-2.5kb center 2.5kb
0 5 10
0 5 10
0 5 10
0 5 10
Normalized ChIP-seq Signal
E
Day2 iCLMs
GMT
GHMT
AGHMT
(%)
25
20
15
10
5
0
< -500
-500 to -50
-50 to -5
-5 to 0
0 to 5
5 to 50
50 to 500
> 500
TF Peak Distance to TSS (kb)
C
Day2 GMT iCLMs
cell–substrate adhesion (174)
positive regulation of cellular component biogenesis (166)
regulation of actin filament–based process (189)
cell junction organization (153)
cardiac muscle tissue development (99)
protein import (153)
regulation of binding (132)
nucleocytoplasmic transport (179)
nuclear import (136)
protein localization to cell periphery (103)
cellular response to organonitrogen compound (80)
cell–substrate adherens junction assembly (32)
focal adhesion assembly (32)
muscle cell differentiation (70)
adherens junction organization (38)
cellular response to peptide (45)
cell–cell junction organization (39)
muscle system process (62)
mitotic nuclear division (71)
actin filament organization (59)
positive regulation of intracellular protein transport (23)
mitotic cell cycle phase transition (26)
actomyosin structure organization (18)
cell surface receptor signaling pathway involved in cell–cell signaling (32)
positive regulation of NFAT protein import into nucleus (5)
single–organism nuclear import (23)
positive regulation of cellular protein localization (27)
cell cycle phase transition (26)
protein import into nucleus (22)
protein targeting to nucleus (22)
p-value
1.0e–05
7.5e–06
5.0e–06
2.5e–06
Percentage
0.25
0.50
0.75
1.00
TF occupancy
1
2
3
D
Day2 GHMT iCLMs
cell–cell junction organization (160)
negative regulation of cell–substrate adhesion (96)
actin filament organization (286)
muscle system process (227)
negative regulation of phosphorylation (262)
cellular response to hormone stimulus (191)
regulation of protein serine/threonine kinase activity (171)
negative regulation of protein phosphorylation (170)
negative regulation of locomotion (124)
cardiac muscle tissue development (273)
muscle cell differentiation (233)
regulation of actin filament–based process (202)
regulation of intracellular transport (128)
mRNA processing (109)
regulation of intracellular protein transport (100)
heart morphogenesis (75)
in utero embryonic development (112)
regulation of actin cytoskeleton organization (109)
actomyosin structure organization (80)
cardiocyte differentiation (52)
response to transforming growth factor beta (84)
muscle cell development (66)
striated muscle cell development (61)
nucleocytoplasmic transport (73)
striated muscle cell differentiation (86)
protein import into nucleus (56)
protein targeting to nucleus (56)
nuclear transport (73)
single–organism nuclear import (56)
protein import (62)
nuclear import (56)
ellular response to transforming growth factor beta stimulus (26)
regulation of Ras protein signal transduction (23)
transforming growth factor beta receptor signaling pathway (19)
regulation of cytoskeleton organization (37)
positive regulation of supramolecular fiber organization (20)
regulation of supramolecular fiber organization (28)
p-value
3e–06
2e–06
1e–06
Percentage
0.25
0.50
0.75
1.00
TF occupancy
1
2
3
4

Figure S2, related to Figure 1. Genome-wide Co-occupancy of Reprogramming Factors in GMT and GHMT iCLMs.

(A,B) ChIP-seq data for Gata4, Mef2c, and Tbx5 reveals co-occupancy at 14,106 genomic binding sites 2 days following GMT-mediated reprograming of MEFs (A). ChIP-seq data for Gata4, Mef2c, Hand2, and Tbx5 reveals co-occupancy at 25,512 genomic binding sites 2 days following GHMT-mediated reprograming of MEFs (B). Normalized ChIP-seq binding profiles for TF in each cluster are shown.

(C,D) Each TF peak in GMT (C) or GHMT (D) MEF iCLMs was annotated to the nearest neighboring gene. GO enrichment analysis for biological process was performed with DAVID (v6.8). clusterProfiler (v3.6.0) was used to visualize GO term enrichment from different groups based on the number of occupying TFs. Terms related to heart or muscle are highlighted in red.

(E) Percentage of TF peaks in GMT, GHMT, and AGHMT iCLMs categorized by the distance to TSS.

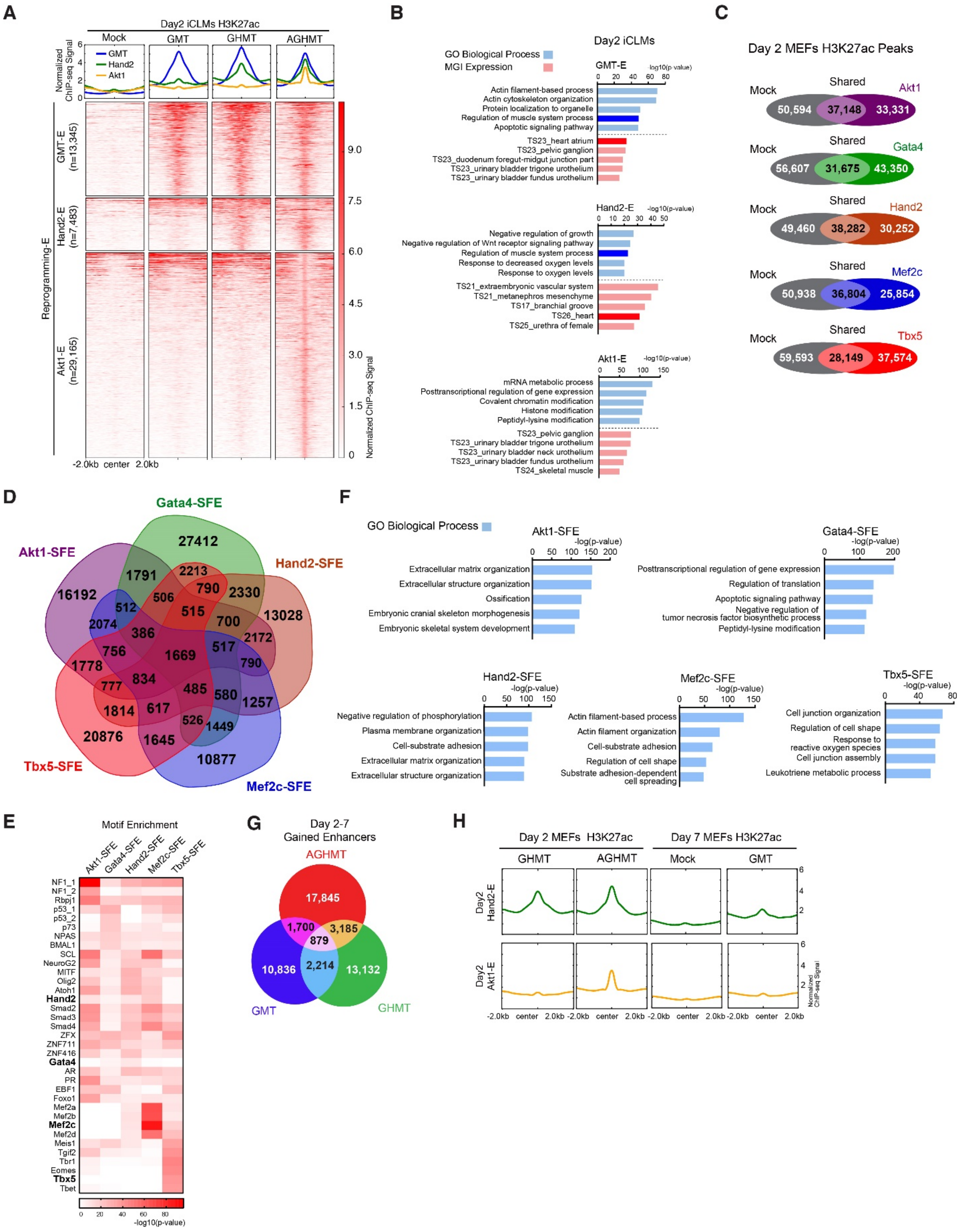
A
Day2 iCLMs H3K27ac
Mock
GMT
GHMT
AGHMT
GMT
Hand2
Akt1
Normalized ChIP-seq Signal
Reprogramming-E
GMT-E (n=13,345)
Hand2-E (n=7,483)
Akt1-E (n=29,165)
-2.0kb center 2.0kb
9.0
7.5
6.0
4.5
3.0
1.5
0
Normalized ChIP-seq Signal
B
Day2 iCLMs
GO Biological Process
MGI Expression
GMT-E
-log10(p-value)
Actin filament-based process
Actin cytoskeleton organization
Protein localization to organelle
Regulation of muscle system process
Apoptotic signaling pathway
TS23_heart atrium
TS23_pelvic ganglion
TS23_duodenum foregut-midgut junction part
TS23_urinary bladder trigone urothelium
TS23_urinary bladder fundus urothelium
Hand2-E
Negative regulation of growth
Negative regulation of Wnt receptor signaling pathway
Regulation of muscle system process
Response to decreased oxygen levels
Response to oxygen levels
TS21_extraembryonic vascular system
TS21_metanephros mesenchyme
TS17_branchial groove
TS26_heart
TS25_urethra of female
Akt1-E
mRNA metabolic process
Posttranscriptional regulation of gene expression
Covalent chromatin modification
Histone modification
Peptidyl-lysine modification
TS23_pelvic ganglion
TS23_urinary bladder trigone urothelium
TS23_urinary bladder neck urothelium
TS23_urinary bladder fundus urothelium
TS24_skeletal muscle
C
Day 2 MEFs H3K27ac Peaks
Mock Shared Akt1 50,594 37,148 33,331
Mock Shared Gata4 56,607 31,675 43,350
Mock Shared Hand2 49,460 38,282 30,252
Mock Shared Mef2c 50,938 36,804 25,854
Mock Shared Tbx5 59,593 28,149 37,574
D
Gata4-SFE
Akt1-SFE
Hand2-SFE
Tbx5-SFE
Mef2c-SFE
27412
16192
13028
20876
10877
1791
2213
790
2330
506
512
515
700
2074
386
2172
756
1669
517
790
1778
834
777
485
580
1257
1814
617
526
1449
1645
F
GO Biological Process
Akt1-SFE
-log(p-value)
Extracellular matrix organization
Extracellular structure organization
Ossification
Embryonic cranial skeleton morphogenesis
Embryonic skeletal system development
Gata4-SFE
Posttranscriptional regulation of gene expression
Regulation of translation
Apoptotic signaling pathway
Negative regulation of tumor necrosis factor biosynthetic process
Peptidyl-lysine modification
Hand2-SFE
Negative regulation of phosphorylation
Plasma membrane organization
Cell-substrate adhesion
Extracellular matrix organization
Extracellular structure organization
Mef2c-SFE
Actin filament-based process
Actin filament organization
Cell-substrate adhesion
Regulation of cell shape
Substrate adhesion-dependent cell spreading
Tbx5-SFE
Cell junction organization
Regulation of cell shape
Response to reactive oxygen species
Cell junction assembly
Leukotriene metabolic process
E
Motif Enrichment
Akt1-SFE
Gata4-SFE
Hand2-SFE
Mef2c-SFE
Tbx5-SFE
NF1_1
NF1_2
Rbpj1
p53_1
p53_2
p73
NPAS
BMAL1
SCL
NeuroG2
MITF
Olig2
Atoh1
Hand2
Smad2
Smad3
Smad4
ZFX
ZNF711
ZNF416
Gata4
AR
PR
EBF1
Foxo1
Mef2a
Mef2b
Mef2c
Mef2d
Meis1
Tgif2
Tbr1
Eomes
Tbx5
Tbet
0 20 40 60 80
-log10(p-value)
G
Day 2-7 Gained Enhancers
AGHMT
GMT
GHMT
17,845
1,700
3,185
879
10,836
2,214
13,132
H
Day 2 MEFs H3K27ac
Day 7 MEFs H3K27ac
GHMT
AGHMT
Mock
GMT
Day2 Hand2-E
Day2 Akt1-E
-2.0kb center 2.0kb
Normalized ChIP-seq Signal

Figure S3, related to Figure 2. Reprogramming Enhancer Activation Requires Cooperative Actions of Reprogramming Factors.

(A) Heatmap of H3K27ac ChIP-seq signals in Reprogramming-E peaks for day 2 Mock-infected MEFs, GMT-, GHMT-, or AGHMT-iCLMs using a 4kb-window. H3K27ac ChIP-seq signals in the Reprogramming-E peaks from (Figure 2A) were clustered into three groups depending on their response to GMT (GMT-E), GHMT (Hand2-E), and AGHMT (Akt1-E). Normalized ChIP-seq binding profiles for H3K27ac in each cluster are shown.

(B) H3K27ac enhancer peaks of day 2 reprogramming enhancers were functionally annotated using GREAT. Five of the most overrepresented terms belonging to the GO Biological Process (blue) and MGI Expression (red) in each enhancer cluster are shown. Terms related to heart or muscle are highlighted in dark colors.

(C) Venn diagrams showing the number of overlapping H3K27ac enhancer peaks between Mock and each single factor overexpressing MEFs.

(D) Venn diagram showing the number of overlapping H3K27ac peaks among each SFE region.

(E) Heatmap of known motifs enriched in each SFE region. Reprogramming TFs are in bold.

(F) H3K27ac peaks of each single factor overexpressing MEFs were functionally annotated using GREAT. Five of the most overrepresented terms belonging to the GO Biological Process are shown.

(G) Venn diagrams showing the number of overlapping H3K27ac peaks of gained enhancers between day 2 and 7 in GMT, GHMT, and AGHMT iCLMs.

(H) Normalized ChIP-seq binding profiles for H3K27ac in day 2 GHMT and AGHMT iCLMs and day 7 Mock and GMT iCLMs at day 2 Hand2-E and Akt1-E regions from (A).

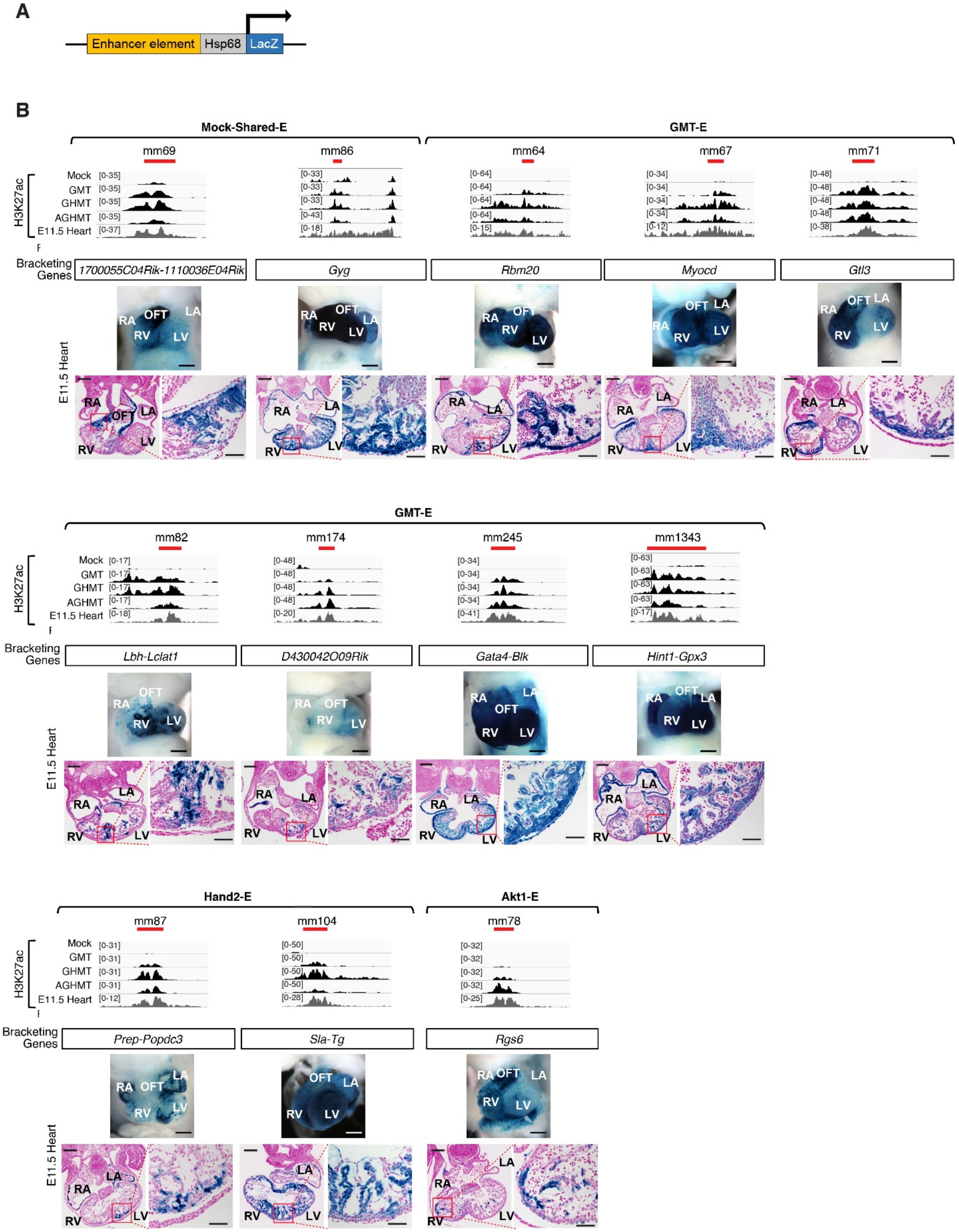
A
Enhancer element
Hsp68
LacZ
B
Mock-Shared-E
GMT-E
mm69
mm86
mm64
mm67
mm71
H3K27ac
Mock
GMT
GHMT
AGHMT
E11.5 Heart
Bracketing Genes
1700055C04Rik-1110036E04Rik
Gyg
Rbm20
Myocd
Gtl3
E11.5 Heart
RA
OFT
LA
RV
LV
GMT-E
mm82
mm174
mm245
mm1343
Lbh-Lclat1
D430042O09Rik
Gata4-Blk
Hint1-Gpx3
Hand2-E
Akt1-E
mm87
mm104
mm78
Prep-Popdc3
Sla-Tg
Rgs6

Figure S4, related to Figure 4. iCLM Enhancers Display Specific Expression Patterns in the Developing Heart.

(A) Schematic of Hsp68-LacZ construct for transgenic enhancer reporter assay.

(B) Cardiac subregional specificities of additional iCLM enhancers as shown in Figure 4B. (Black scale bars: 500μm for whole mount heart, 200μm and 50μm for low and high magnification histology sections, respectively)

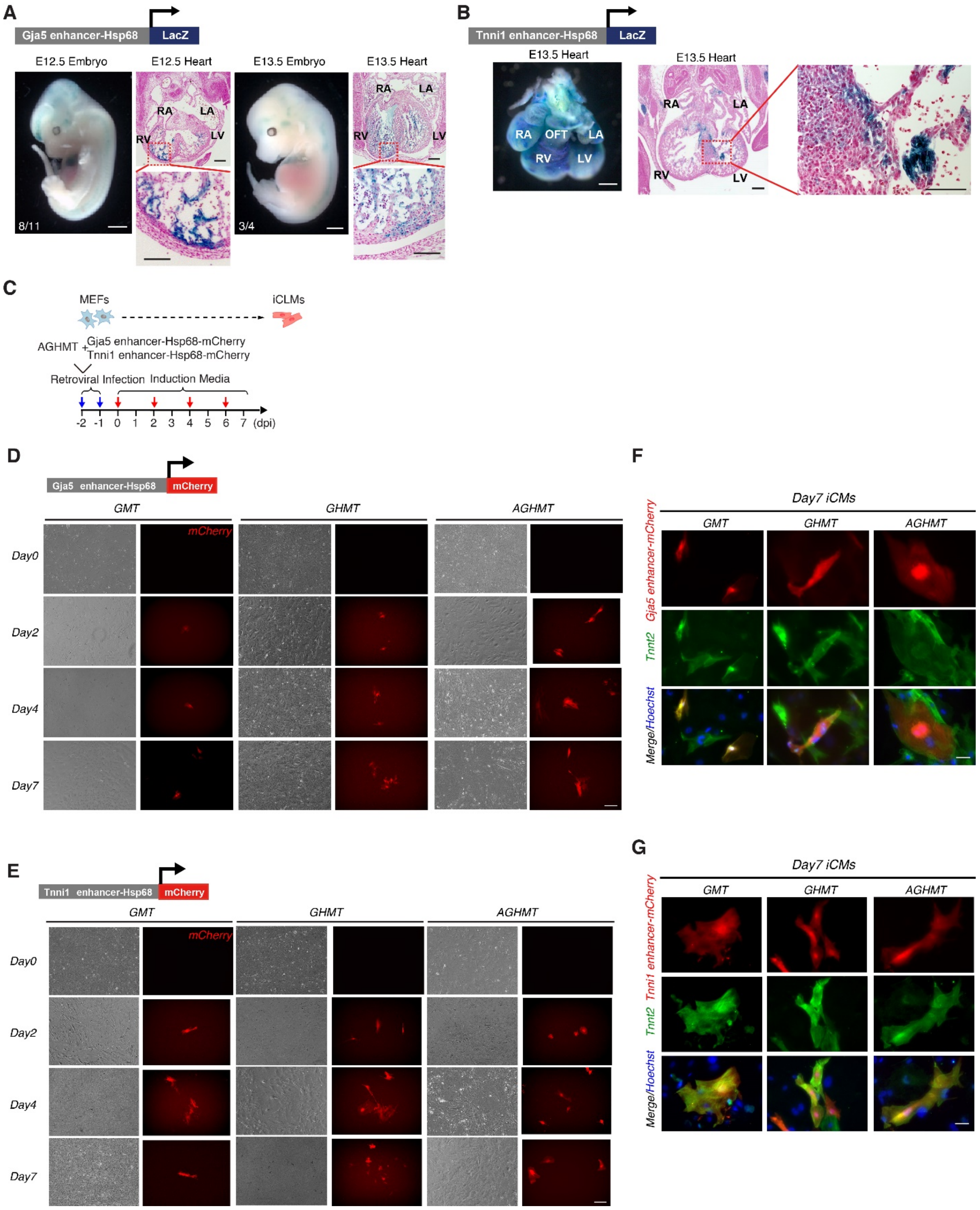
A
Gja5 enhancer-Hsp68
LacZ
E12.5 Embryo
E12.5 Heart
E13.5 Embryo
E13.5 Heart
RA
LA
RV
LV
8/11
3/4
B
Tnni1 enhancer-Hsp68
LacZ
E13.5 Heart
E13.5 Heart
RA
OFT
LA
RV
LV
C
MEFs
iCLMs
AGHMT +
Gja5 enhancer-Hsp68-mCherry
Tnni1 enhancer-Hsp68-mCherry
Retroviral Infection
Induction Media
-2 -1 0 1 2 3 4 5 6 7 (dpi)
D
Gja5 enhancer-Hsp68
mCherry
GMT
GHMT
AGHMT
mCherry
Day0
Day2
Day4
Day7
E
Tnni1 enhancer-Hsp68
mCherry
GMT
GHMT
AGHMT
mCherry
Day0
Day2
Day4
Day7
F
Day7 iCMs
GMT
GHMT
AGHMT
Gja5 enhancer-mCherry
Tnnt2
Merge/Hoechst
G
Day7 iCMs
GMT
GHMT
AGHMT
Tnni1 enhancer-mCherry
Tnnt2
Merge/Hoechst

Figure S5, related to Figure 4. Putative *Gja5* and *Tnni1* Enhancer Activity at Different Stages of Embryonic Development and Reprogramming.

(A) Gross images of Gja5-E-Hsp68-LacZ transgenic whole embryos stained with β–galactosidase at E12.5 and E13.5. Section of E12.5 and E13.5 Gja5-E-Hsp68-LacZ transgenic heart counter-stained with Nuclear Fast Red showing expression of LacZ in the myocardium. Numbers indicate embryos with cardiac expression over the total LacZ+ genotyped embryos. (White scale bars: 1mm, Black scale bars: 200μm and 50μm for low and high magnification histology sections, respectively).

(B) Representative image of Tnni1-E-Hsp68-LacZ E13.5 transgenic heart stained with β-galactosidase showing LacZ expression in the heart (White scale bar: 500μm). Section of Tnni1-E-Hsp68-LacZ E13.5 transgenic heart stained with Nuclear Fast Red showing LacZ expression in the myocardium (Black scale bars: 200μm and 50μm for low and high magnification histology sections, respectively).

(C) Strategy for testing enhancer activity during direct cardiac reprogramming in MEFs. Gja5-E-Hsp68-mCherry or Tnni1-E-Hsp68-mCherry was retrovirally delivered to MEFs along with the reprogramming factors. (dpi, days post induction)

(D,E) Representative live cell images of day 0, 2, 4 and 7 Gja5-E-Hsp68-mCherry (D) or Tnni1-E-Hsp68-mCherry (E) iCLMs in different reprogramming cocktails showing mCherry expression. (Bars, 200μm).

(F,G) Representative immunocytochemistry images of GMT, GHMT and AGHMT iCLMs expressing mCherry under Gja5-E (F) or Tnni1-E (G) activity. Cells were fixed and stained for Tnnt2 (green), mCherry (red), and Hoechst (blue) 7 days after infection. (Bars, 50μm).

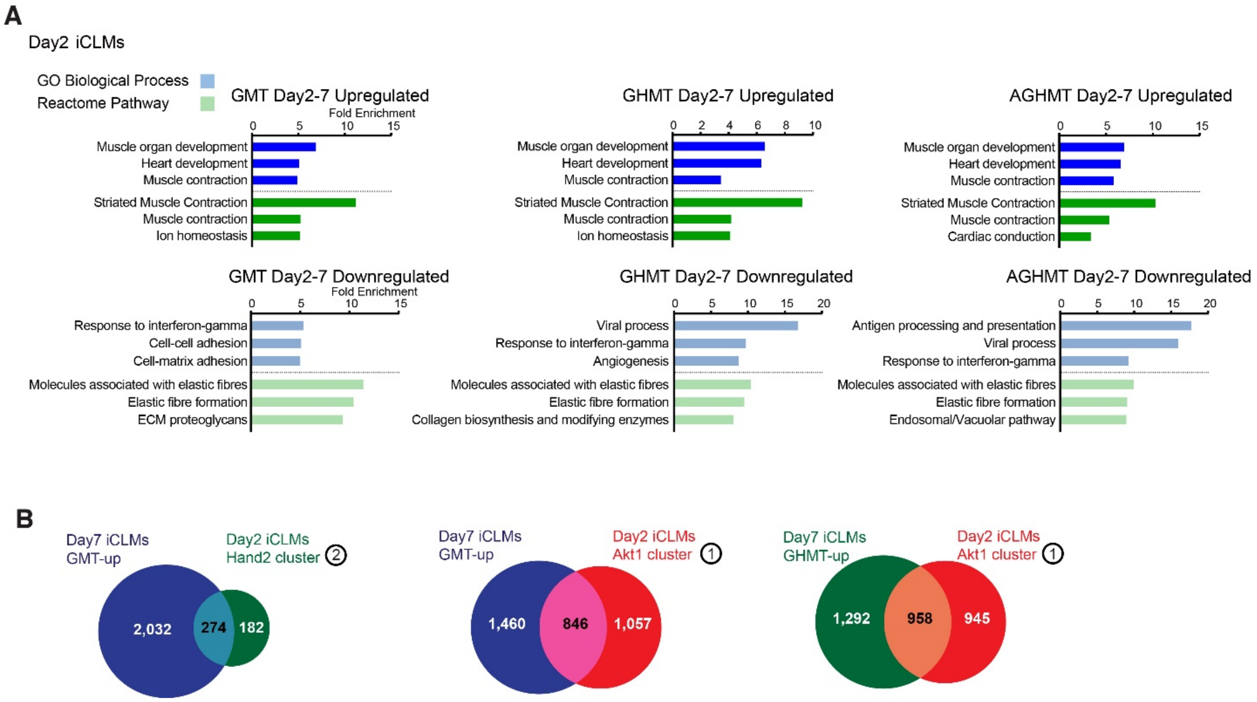

Figure S6, related to Figure 5. Time Dependent Activation of Cardiac Genes during Cardiac Reprogramming.

(A) Functional annotation of gene sets changing between day 2 and 7 iCLMs was performed by PANTHER and the three most overrepresented GO Biological Process (blue) and Reactome Pathway (green) terms are shown. Gene sets upregulated show high enrichment of terms related to heart or muscle development and contraction, which are highlighted in dark colors.

(B) Venn diagrams showing the number of overlapping genes between the upregulated genes in day 7 GMT and GHMT iCLMs with day 2 iCLM Hand2 and Akt1 cluster from (Figure 5E).

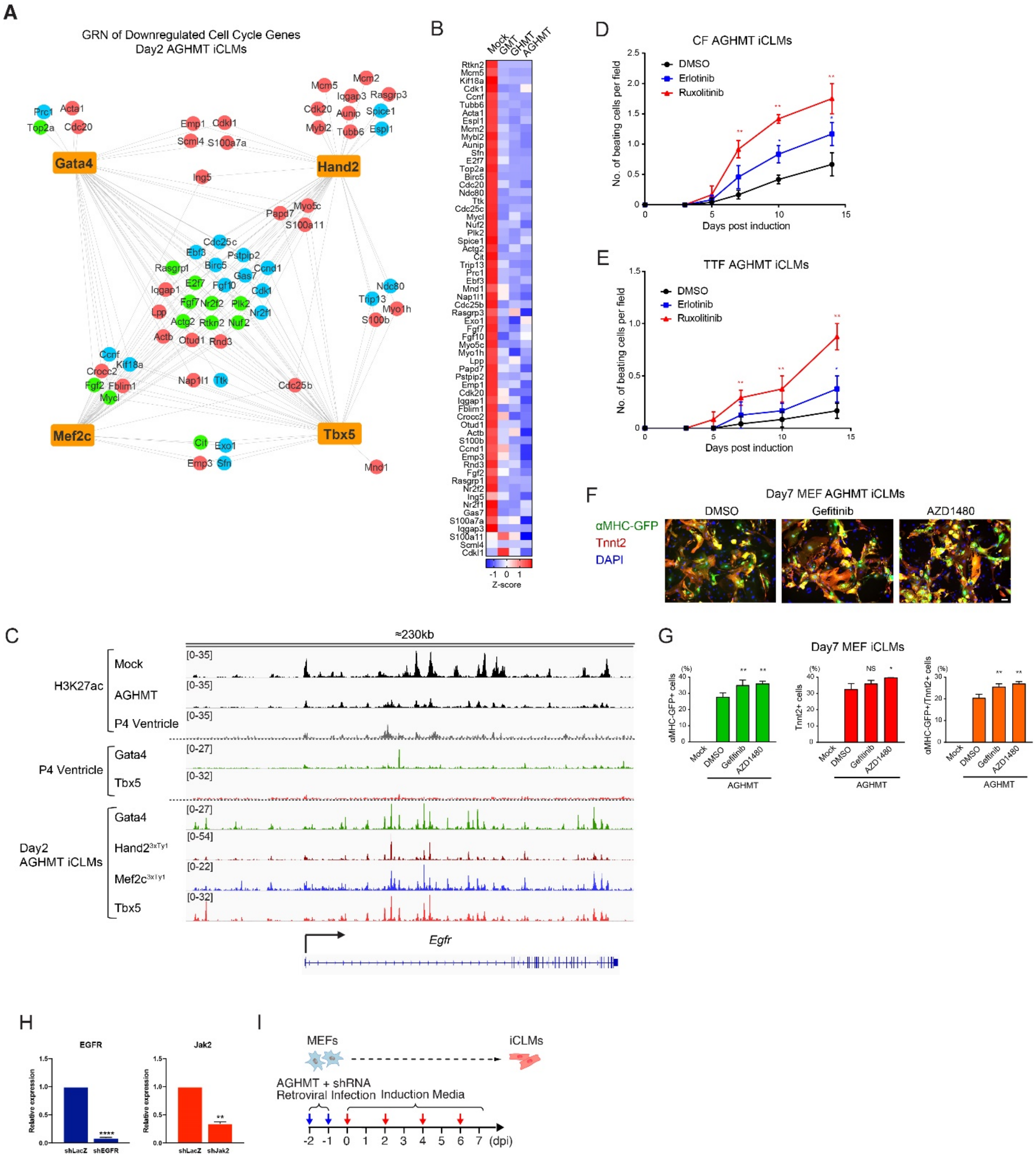
A
GRN of Downregulated Cell Cycle Genes
Day2 AGHMT iCLMs
Gata4
Hand2
Mef2c
Tbx5
Prc1
Acta1
Top2a
Cdc20
Emp1
Cdkl1
Scml4
S100a7a
Mcm5
Mcm2
Iqgap3
Rasgrp3
Cdk20
Aunip
Spice1
Mybl2
Tubb6
Espl1
Ing5
Myo5c
Papd7
S100a11
Cdc25c
Ebf3
Pstpip2
Rasgrp1
Birc5
Ccnd1
Gas7
Iqgap1
E2f7
Fgf10
Cdk1
Lpp
Fgf7
Nr2f2
Plk2
Nr2f1
Actg2
Rtkn2
Nuf2
Actb
Otud1
Rnd3
Ndc80
Trip13
Myo1h
S100b
Ccnf
Kif18a
Crocc2
Fgf2
Fblim1
Mycl
Nap1l1
Ttk
Cdc25b
Cit
Exo1
Emp3
Sfn
Mnd1
B
Mock
GMT
GHMT
AGHMT
Rtkn2
Mcm5
Kif18a
Cdk1
Ccnf
Tubb6
Acta1
Espl1
Mcm2
Mybl2
Aunip
Sfn
E2f7
Top2a
Birc5
Cdc20
Ndc80
Ttk
Cdc25c
Mycl
Nuf2
Plk2
Spice1
Actg2
Cit
Trip13
Prc1
Ebf3
Mnd1
Nap1l1
Cdc25b
Rasgrp3
Exo1
Fgf7
Fgf10
Myo5c
Myo1h
Lpp
Papd7
Pstpip2
Emp1
Cdk20
Iqgap1
Fblim1
Crocc2
Otud1
Actb
S100b
Ccnd1
Emp3
Rnd3
Fgf2
Rasgrp1
Nr2f2
Ing5
Nr2f1
Gas7
S100a7a
Iqgap3
S100a11
Scml4
Cdkl1
-1 0 1
Z-score
C
≈230kb
H3K27ac
Mock
AGHMT
P4 Ventricle
[0-35]
[0-35]
[0-35]
P4 Ventricle
Gata4
Tbx5
[0-27]
[0-32]
Day2 AGHMT iCLMs
Gata4
Hand2^3xTy1
Mef2c^3xTy1
Tbx5
[0-27]
[0-54]
[0-22]
[0-32]
Egfr
D
CF AGHMT iCLMs
DMSO
Erlotinib
Ruxolitinib
No. of beating cells per field
2.5
2.0
1.5
1.0
0.5
0
0
5
10
15
Days post induction
**
**
**
*
*
E
TTF AGHMT iCLMs
DMSO
Erlotinib
Ruxolitinib
No. of beating cells per field
1.5
1.0
0.5
0
0
5
10
15
Days post induction
**
**
**
*
F
Day7 MEF AGHMT iCLMs
αMHC-GFP
Tnnt2
DAPI
DMSO
Gefitinib
AZD1480
G
Day7 MEF iCLMs
αMHC-GFP+ cells
(%)
40
30
20
10
0
**
**
Mock
DMSO
Gefitinib
AZD1480
AGHMT
Tnnt2+ cells
(%)
40
30
20
10
0
NS
*
Mock
DMSO
Gefitinib
AZD1480
AGHMT
αMHC-GFP+/Tnnt2+ cells
(%)
30
20
10
0
**
**
Mock
DMSO
Gefitinib
AZD1480
AGHMT
H
EGFR
Relative expression
1.5
1.0
0.5
0.0
****
shLacZ
shEGFR
Jak2
Relative expression
1.5
1.0
0.5
0.0
**
shLacZ
shJak2
I
MEFs
iCLMs
AGHMT + shRNA
Retroviral Infection
Induction Media
-2
-1
0
1
2
3
4
5
6
7
(dpi)

Figure S7, related to Figure 7. Suppression of Cell Cycle Related Genes during Reprogramming.

(A) GRN of downregulated cell cycle pathway genes in day 2 AGHMT iCLMs. Each node represents a gene and edges are drawn to all the annotated genes of reprogramming TF peaks.

(B) Gene expression heatmap of all genes from (A).

(C) A genome browser view of the *Egfr* locus showing multiple unique TF peaks and dampening of H3K27ac signal in AGHMT iCLMs.

(D,E) Quantification of spontaneous beating CF (D) and TTF (E) iCLMs after treatment (n=3, independent experiments). (* $P < 0.05$ vs. AGHMT+DMSO, ** $P < 0.01$ vs. AGHMT+DMSO). Data represented as mean ± SD.

(F) Representative immunocytochemistry images of AGHMT reprogrammed fibroblasts from αMHC-GFP transgenic mice treated with DMSO or the indicated chemicals. Cells were fixed and stained for αMHC-GFP (green), Tnnt2 (red), and DAPI (blue) 7 days after infection. (Bars, 100μm).

(G) Quantification by flow cytometry of αMHC-GFP+ and Tnnt2+ iCLMs 7 days after treatment with AGHMT and DMSO or the indicated chemicals (n=3, independent experiments). (* $P < 0.05$ vs. AGHMT+DMSO, ** $P < 0.01$ vs. AGHMT+DMSO). Data represented as mean ± SD.

(H) Suppression of *Egfr* and *Jak2* transcript levels in MEFs 2 days after infection of shRNAs (n=3, independent experiments). Transcript levels are normalized to 18S. (** $P < 0.01$ vs. shLacZ, **** $P < 0.0001$ vs. shLacZ). Data represented as mean ± SD.

(I) Strategy for knockdown by shRNA during direct cardiac reprogramming in MEFs. shRNAs were retrovirally delivered to MEFs together with the reprogramming factors. (dpi, days post induction).

Table S1, related to Figures 1 and S2. Summary of TF occupancy in day2 iCLMs.

	GMT	GHMT	AGHMT
Single	9372 (66.9%)	13660 (53.6%)	20868 (50.2%)
Two	3584 (25.6%)	6657 (26.1%)	11037 (26.5%)
Three	1054 (7.5%)	3743 (14.7%)	6791 (16.3%)
Four	-	1447 (5.7%)	2900 (7.0%)
Total	14010	25507	41596

TF Peaks with single TF occupancy

	GMT	GHMT	AGHMT
Gata4	1613 (17.2%)	1769 (13.0%)	7037 (33.7%)
Hand2	-	4531 (33.2%)	5901 (28.3%)
Mef2c	3362 (35.9%)	2506 (18.3%)	2125 (10.2%)
Tbx5	4397 (46.9%)	4854 (35.5%)	5805 (27.8%)
Total	9372	13660	20868

TF Peaks with two TF occupancy

	GMT	GHMT	AGHMT
GM	480 (13.4%)	332 (5.0%)	786 (7.1%)
GT	1663 (46.4%)	1260 (19.0%)	4471 (40.5%)
MT	1441 (40.2%)	838 (12.6%)	781 (7.1%)
GH	-	859 (12.9%)	1609 (14.6%)
HM	-	1011 (15.2%)	584 (5.3%)
HT	-	2357 (35.4%)	2806 (25.4%)
Total	3584	6657	11037

TF Peaks with three TF occupancy

	GMT	GHMT	AGHMT
GMT	1054 (100%)	383 (10.2%)	1294 (19.1%)
GHM	-	352 (9.4%)	421 (6.2%)
GHT	-	1793 (47.9%)	4401 (64.8%)
HMT	-	1215 (32.5%)	675 (9.9%)
Total	1054	3743	6791

TF Peaks with four TF occupancy

	GMT	GHMT	AGHMT
GHMT	-	1447	2900

Table S2, related to Figure 2. Known motifs recovered from reprogramming enhancers in day 2 iCLMs. Percent of target describes the frequency of motifs discovered at the target sites. Reprogramming TFs are highlighted in bold.

Symbol	Motif	GMT-Enhancer P-Value	GMT-Enhancer % of Targets	Hand2-Enhancer P-Value	Hand2-Enhancer % of Targets	Akt1-Enhancer P-Value	Akt1-Enhancer % of Targets
Nfib	NF1-halfsite(CTF)	1.00E-14	18.54	1.00E-09	20.41	1.00E-20	18.55
Meis1	Meis1(Homeobox)	1.00E-15	20.24	0.001	20.23	1.00E-17	19.31
Tgif1	Tgif1(Homeobox)	1.00E-14	36.1	1.00E-06	36.62	1.00E-17	34.45
Tgif2	Tgif2(Homeobox)	1.00E-11	37.48	1.00E-08	38.69	1.00E-14	36.33
Smad2	Smad2(MAD)	1.00E-13	17.11	1.00E-08	19.79	1.00E-14	16.4
Smad3	Smad3(MAD)	1.00E-12	32.49	1.00E-07	36.67	1.00E-08	31.42
Smad4	Smad4(MAD)	1.00E-16	17.4	1.00E-11	20.61	1.00E-13	16.74
Mef2a	Mef2a(MADS)	1.00E-122	8.22	1.00E-27	6.16	1.00E-24	4.56
Mef2b	Mef2b(MADS)	1.00E-160	14.56	1.00E-34	11.47	1.00E-36	8.94
Mef2c	**Mef2c(MADS)**	**1.00E-132**	**8.82**	**1.00E-38**	**6.8**	**1.00E-31**	**5.04**
Mef2d	Mef2d(MADS)	1.00E-104	4.69	1.00E-26	3.07	1.00E-29	2.29
Ar	AR-halfsite(NR)	1.00E-11	42	0.001	46.64	1.00E-16	42.48
Stat4	STAT4(Stat)	0.0001	10.16	1.00E-06	11.29	0.001	9.94
Tbx5	**Tbx5(T-box)**	**1.00E-16**	**34.43**	**1.00E-06**	**36.86**	**0.001**	**32.28**
Gata3	GATA3(Zf)	1.00E-65	21.27	1.00E-31	20.01	0.001	15.29
Gata1	Gata1(Zf)	1.00E-34	8.45	1.00E-20	7.95	0.001	5.75
Gata4	**Gata4(Zf)**	**1.00E-51**	**14.39**	**1.00E-25**	**13.4**	**1.00E-06**	**10.17**
Gata6	Gata6(Zf)	1.00E-56	13.43	1.00E-26	12.37	1.00E-06	9.35
Zfp711	ZNF711(Zf)	1.00E-07	14.64	0.0001	17.67	1.00E-28	16.42
Zfx	ZFX(Zf)	1.00E-08	11.86	1.00E-05	13.75	1.00E-33	13.26
Atoh1	Atoh1(bHLH)	1.00E-06	11.29	1.00E-15	14.25	1.00E-11	11.66
Hand2	**Hand2(bHLH)**	**1.00E-13**	**6.19**	**1.00E-20**	**7.58**	**1.00E-09**	**5.53**
Myod1	MyoD(bHLH)	0.0001	7.9	1.00E-07	8.67	0.001	7.94
Neurod1	NeuroD1(bHLH)	0.0001	8.36	1.00E-07	10.44	1.00E-07	8.48
Neurog2	NeuroG2(bHLH)	1.00E-07	16.52	1.00E-11	19.66	1.00E-13	16.8
Olig2	Olig2(bHLH)	1.00E-07	20.91	1.00E-07	24.51	1.00E-09	20.65
Tal1	SCL(bHLH)	1.00E-08	46.44	1.00E-05	51.33	1.00E-20	47.33
Tfap4	Ap4(bHLH)	1.00E-07	12.84	0.0001	14.49	1.00E-07	12.83
Rbpj	Rbpj1	1.00E-09	15.55	1.00E-07	16.74	1.00E-05	15.02

Table S3, related to Figure 2. Known motifs recovered from enhancers gained by day 7 compared to day 2 iCLMs. Percentage of targets describes the frequency of motifs discovered at the target sites. Reprogramming TFs are highlighted in bold.

Symbol	Motif	GMT P-Value	GMT % of Targets	GHMT P-Value	GHMT % of Targets	AGHMT P-Value	AGHMT % of Targets
Ar	AR-halfsite(NR)	1.00E-05	36.83	1.00E-05	37.7	1.00E-05	36
Bapx1	Bapx1(Homeobox)	0.1	19.66	1	19.72	1.00E-06	20.05
Nr2f2	COUP-TFII(NR)	0.01	14.11	0.01	14.54	1.00E-06	14.02
Ctcf	CTCF(Zf)	1.00E-09	1.06	0.1	0.83	0.1	0.61
Esrra	Erra(NR)	1.00E-06	18.62	1.00E-06	19.14	1.00E-06	18.13
Esrrb	Esrrb(NR)	1.00E-05	5.96	0.0001	5.89	1.00E-09	5.92
Gata1	Gata1(Zf)	1.00E-06	6.66	1.00E-05	6.19	0.01	6.03
Gata2	Gata2(Zf)	0.0001	7.45	1.00E-05	7.13	0.01	6.92
Gata4	**Gata4(Zf)**	**1.00E-07**	**11.86**	**0.001**	**10.92**	**0.001**	**11.2**
Gata6	Gata6(Zf)	1.00E-06	10.96	0.01	9.92	0.01	10.15
Mef2a	Mef2a(MADS)	1.00E-18	5.84	1.00E-29	5.69	1.00E-35	6.16
Mef2b	Mef2b(MADS)	1.00E-35	11.49	1.00E-27	10.62	1.00E-50	11.82
Mef2c	**Mef2c(MADS)**	**1.00E-35**	**6.9**	**1.00E-28**	**6.04**	**1.00E-38**	**6.73**
Mef2d	Mef2d(MADS)	1.00E-31	3.23	1.00E-20	2.88	1.00E-32	3.14
Nfib	NF1(CTF)	0.001	2.76	1.00E-06	2.96	0.1	2.4
Sox15	Sox15(HMG)	1	11.35	1	10.99	1.00E-09	12.08
Thrb	THRb(NR)	1.00E-05	36.81	1.00E-08	37.7	1.00E-09	36.58
Tlx1	Tlx(NR)	1.00E-08	3.45	0.01	3.47	1	2.77
Zfp418	ZNF416(Zf)	0.0001	10.99	0.1	10.98	1.00E-07	10.55

Table S5, related to Figures 4 and S4. List of VISTA mouse elements and Reprogramming Enhancers used to confirm *in vivo* cardiac activity by LacZ transgenic mouse assay.

Enhancer ID	Enhancer coordinates (mm10)	Enhancer length(bp)	Enhancer activation dependence	TF co-occupancy dependence	Bracketing genes
mm64	chr19:53715915-53717934	2019	GMT	GMT	Rbm20 (intragenic)
mm67	chr11:65207498-65210380	2882	GMT	GMT	Myocd (intragenic)
mm69	chr9:64044784-64046949	2165	GMT	GMT	1700055C04Rik-1110036E04Rik
mm71	chr8:95426508-95428314	1806	GMT	GMT	Gtl3 (intragenic)
mm72	chr3:152304130-152305473	1343	Mock	GMT	Fam73a (intragenic)
mm78	chr12:83072395-83074413	2018	Akt1	Hand2	Rgs6 (intragenic)
mm82	chr17:73022163-73024151	1988	GMT	GMT	Lbh-Lclat1
mm86	chr3:20145236-20146308	1072	Mock	GMT	Gyg (intragenic)
mm87	chr10:45228613-45231786	3173	Hand2	GMT	Prep-Popdc3
mm104	chr15:66824301-66827162	2861	Hand2	GMT	Sla-Tg
mm130	chr9:24887072-24890068	2996	Hand2	Hand2	Tbx20-Herpud2
mm145	chr4:120391603-120393946	2343	GMT	GMT	Foxo6-Scmh1
mm146	chr11:77422469-77424441	1972	GMT	GMT	Ssh2 (intragenic)
mm152	chr18:80330119-80332361	2242	Hand2	Hand2	Kcng2 (intragenic)
mm169	chr7:80445068-80446500	1432	Hand2	Hand2	Furin-Blm
mm174	chr7:125764047-125765353	1306	Hand2	Hand2	D430042O09Rik (intragenic)
mm245	chr14:63367789-63369845	2056	GMT	GMT	Gata4-Blk
mm1343	chr11:54879186-54884157	4971	GMT	GMT	Hint1-Gpx3
Putative Gja5	chr3:97062652-97063357	705	Hand2	Hand2	Gja5-Acp6
Putative Tnni1	chr1:135800059-135801243	1184	GMT	GMT	Tnni1 (intragenic)

Table S6, related to Figures 6 and 7. Number of genes in each cluster of day 2 AGHMT iCLMs GRN.

	Upregulated GRN	Downregulated GRN
Gata4	86	85
Hand2	91	105
Mef2c	31	32
Tbx5	76	77
GM	19	13
GT	107	85
MT	27	10
GH	52	62
HM	28	24
HT	93	64
GMT	70	42
GHM	38	22
GHT	332	265
HMT	56	28
GHMT	700	290
Total	1806	1204